

MULTIBAND HANDSET ANTENNA ANALYSIS INCLUDING LTE BAND MIMO SERVICE

Hyunho Wi, Byeongkwan Kim, Woojae Jung, and Byungje Lee*

Department of Wireless Communications Engineering, Kwangwoon University, 447-1, Wolgye-Dong, Nowon-Gu, Seoul 139-701, Korea

Abstract—A compact multiband handset antenna including MIMO antenna operation for LTE 13 band (746 ~ 787 MHz) applications is proposed. The proposed antennas are separately located on the top and bottom portions of a mobile handset in order to use the antenna area more effectively. The proposed antenna achieves isolations of higher than 14 dB, enveloped correlation coefficients (ECC) of less than 0.25, and total efficiencies of greater than 40%. The operating frequency bands of Antenna 1 and Antenna 2 include the LTE 13 (746 ~ 787 MHz)/DCS/PCS/UMTS (1710 ~ 2170 MHz) bands and the LTE 13 (746 ~ 787 MHz)/GSM850/900 (824 ~ 960 MHz) bands, respectively.

1. INTRODUCTION

Long Term Evolution (LTE) is one of the key technologies in recent mobile wireless communication services. LTE provides improved system capacity and coverage, reliable high peak data rate, and enhanced spectrum efficiency by using a high performance antenna with a multiple-input-multiple-output (MIMO) configuration. By using multiple antennas, MIMO technology provides a good quality of service (QOS) in the multipath environment without additional power [1–3]. It is well-known that achieving high isolation and low Enveloped Correlation Coefficient (ECC) between closely spaced antennas is important in portable MIMO-embedded devices where antennas must be designed within a small volume [4]. However, modern handset antennas should still be miniaturized with good performance, and isolation improvement is also important to realize the MIMO

Received 24 February 2013, Accepted 2 April 2013, Scheduled 14 April 2013

* Corresponding author: Byungje Lee (bj_lee@kw.ac.kr).

antennas for the LTE 700 bands in the limited space of recent mobile handsets [5–7]. Since most MIMO antenna elements of recent mobile handsets are collocated on the same printed circuit board (PCB), the surface current distribution on the PCB induces mutual coupling between antenna elements and common ground plane. Moreover, when mobile handset antennas operate at a lower frequency such as 746 ~ 787 MHz, the MIMO antenna element itself and the ground plane can be similarly operated as two arms of a half wavelength dipole, so that the radiation pattern and isolation between them can be dependent upon the current distribution of the ground plane [8]. Various techniques have been studied for the enhancement of isolation between two closely mounted MIMO antennas [9–15]. An additional coupling element [9, 10] or decoupling network [11, 12] between the two antenna elements is used to improve isolation between the two antennas. Although isolation can be enhanced by artificially generated additional coupling or decoupling current paths, these can be limited on a lower frequency band volume and bandwidth. By properly designing the defected ground structure (DGS) with slots and gaps, a good suppression of mutual coupling between antennas can be achieved [13, 14]. The suspended neutralization line [15], which is physically connected to antenna elements, is also used to improve isolation between MIMO antenna elements. However, applying these techniques for LTE 700 (746 ~ 787 MHz) band MIMO antennas becomes a considerable technical challenge in the industry because of the limited space available to embed such slots and gaps on the ground plane and additional elements between closely packed antennas. While, in most previous studies, all MIMO antenna elements closely stand side-to-side only on the top or bottom portion of a mobile handset, few studies on MIMO antenna configurations have been carried out where the antenna elements are separately located on the top and bottom portions of a mobile handset. Although MIMO antenna elements can also be separated on the top and side portions of a mobile handset, the available side areas of a mobile handset become narrower due to the current trend of a wider screen and larger battery for mobile handsets. Therefore, the MIMO antenna, where antenna elements are separated on the top and bottom portions of a mobile handset, might be an alternative configuration to use the space for the antenna more effectively. In addition to the coverage of frequency bands such as GSM850/GSM900/DCS/PCS/UMTS, operation at the new frequency band (LTE 13 band, 746 ~ 787 MHz) requires a significantly wide impedance bandwidth at a lower frequency band [16–22]. In general, to widen the impedance bandwidth, an additional antenna volume is also needed [23, 24]. The most important issue is how to design compact

multiband antennas in the lower frequency band, and how to obtain good isolation between them with an optimal configuration of MIMO antenna elements.

In this paper, we propose a new configuration of the LTE 13 band MIMO antenna where antenna elements are separately located on the top and bottom portions of a mobile handset. Isolation between them is improved when achieving a diagonally orthogonal radiation pattern by controlling the current path on the ground plane. Finally, we propose two compact antennas for MIMO and multiband operations. The operating frequency bands of Antenna 1 located on the top portion and Antenna 2 located on the bottom portion include the LTE 13 (746 ~ 787 MHz)/DCS/ PCS/UMTS (1710 ~ 2170 MHz) bands and the LTE 13 (746 ~ 787 MHz)/GSM850/900 (824 ~ 960 MHz) bands, respectively.

2. LTE 13 BAND MIMO ANTENNA DESIGN AND ANALYSIS

In this section, isolation enhancement in the LTE 13 band (746 ~ 787 MHz) is studied by reducing the mutual coupling between the MIMO antenna elements and between the MIMO antenna elements and the common ground plane. MIMO antenna elements (MIMO Antenna 1 and MIMO Antenna 2) have the same structure and are separately located on the right sides of the top and bottom portions of a mobile handset, respectively.

Figure 1 shows the geometry of the proposed LTE MIMO antenna. The overall dimension of each MIMO antenna element mounted on a FR-4 ($\epsilon_r = 4.4$, loss tangent = 0.02) substrate is $31 \times 15 \times 6 \text{ mm}^3$, and the size of the ground plane is $60 \times 90 \times 1 \text{ mm}^3$, which corresponds to the 4.3 inch display size of a smart phone. Each MIMO antenna element consists of two radiating elements. One element is the meander line PIFA structure, and the other is the inverted-L shaped structure extended from the ground plane. The separation between the MIMO antenna elements (MIMO Antenna 1 and MIMO Antenna 2) is $0.225\lambda_0$ (90 mm) at 750 MHz. Even though the separation between them is as far as possible within the available space of a mobile handset, the electric distance of this separation is not enough to obtain good isolation using a spatial diversity technique in the lower frequency band. In general, when two linearly polarized antennas are located orthogonal to each other, they can provide polarization diversity by reducing the mutual coupling, so that high isolation and low ECC can be achieved between them [25, 26]. However, this technique with vertical and horizontal polarizations does not work very well for

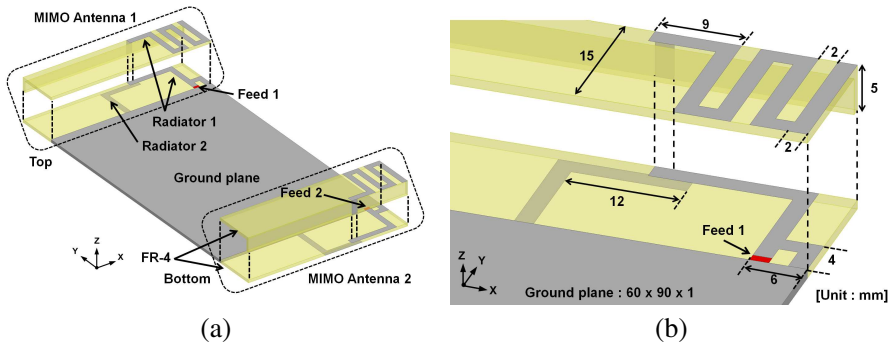


Figure 1. Geometry of LTE MIMO antenna: (a) Overall view and (b) detailed dimensions of MIMO antenna element.

handset antennas in the lower frequency such as the LTE 13 (746 ~ 787 MHz) band because their ground size are usually much smaller than their wavelength ($\lambda_0 = 429$ mm). Therefore, it is necessary to apply alternative techniques for the LTE MIMO handset antenna design.

In this paper, we propose a diagonally orthogonal polarization diversity technique by properly arranging locations of MIMO antenna elements and controlling the ground current path. Figure 2 shows the surface current distribution at 775 MHz when one of MIMO antennas is excited and the other is terminated to a load with 50Ω . It was noticed that while most surface currents are concentrated on the antenna radiating elements themselves (Radiator 1: meander line PIFA structure and Radiator 2: inverted-L shaped structure) and only the small area neighboring them, the currents on MIMO Antenna 2 and most part of the ground plane are barely induced. This is because the inverted-L shaped structure can guide and minimize the area of the surface current distribution on the ground plane, so that mutual coupling between MIMO antenna elements mounted on a common ground plane can be reduced. By also achieving a diagonally orthogonal ground current path as shown in Figure 2(a) with respect to that from MIMO Antenna 2, the mutual coupling between MIMO antenna elements can be minimized since the ground plane of a mobile handset can similarly act as one of the arms of a half wavelength dipole in lower frequency band. Figure 2(b) shows the detailed surface current distribution. L_1 shows the length and direction of the current path on the ground plane, while L_2 and L_3 show the length and direction of the current path on Radiator 1 and Radiator 2, respectively. The overall length ($L_1 + L_2 + L_3$) is about $0.5\lambda_g$ (170 mm) at 775 MHz. By controlling the surface current distribution with Radiator 1 (meander

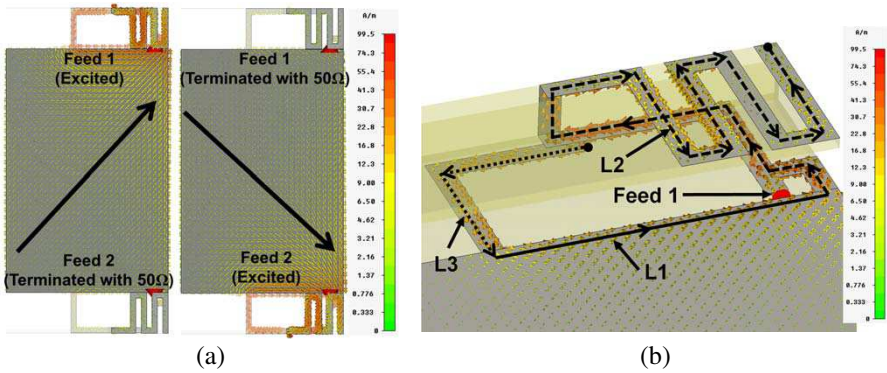


Figure 2. Surface current distribution of MIMO Antenna 1 at 775 MHz: (a) Overall view and (b) detailed view.

line PIFA structure) and Radiator 2 (inverted-L shaped structure), the $0.5\lambda_g$ current path can be concentrated on the right corner of a mobile handset.

Figure 3 shows the simulated results by the MWS CST and measured results of the proposed LTE MIMO antenna. Figure 3(a) shows the simulated and measured S -parameters. The proposed antenna ($VSWR < 3$) covers the entire LTE 13 (746 ~ 787 MHz) band. The measured isolation is higher than 17 dB, and this is generally acceptable for practical mobile handset MIMO antenna applications in the industry. Figure 3(b) shows the simulated and measured radiation patterns at 775 MHz. They have been measured using one antenna that is excited and the other is terminated to a load with $50\ \Omega$. It is noticed that the polarizations of the two antennas are diagonally orthogonal to each other, so that they can provide polarization diversity by reducing the mutual coupling between them. Figure 3(c) shows that the ECC of the proposed LTE MIMO antenna is much less than the recommend value of 0.5. The ECC is obtained by using the far-field radiation patterns as shown in Equation (1) where the incident wave is assumed as the uniform environment ($P(\theta, \phi) = 1$) [27–30].

$$ECC(\rho_e) = \frac{\left| \int_0^{2\pi} \int_0^\pi E_1^*(\theta, \phi) \cdot E_2(\theta, \phi) \cdot P(\theta, \phi) \sin(\theta) d\theta d\phi \right|^2}{\left[\int_0^{2\pi} \int_0^\pi E_1^*(\theta, \phi) \cdot E_1(\theta, \phi) \cdot P(\theta, \phi) \sin(\theta) d\theta d\phi \right] \cdot \left[\int_0^{2\pi} \int_0^\pi E_2^*(\theta, \phi) \cdot E_2(\theta, \phi) \cdot P(\theta, \phi) \sin(\theta) d\theta d\phi \right]} \quad (1)$$

where $E_{1,2}(\theta, \phi)$ is the electric field pattern of antennas 1 and 2, respectively, and $P(\theta, \phi)$ is the incident field angular density function. Figure 3(d) shows the photo of fabricated MIMO antenna.

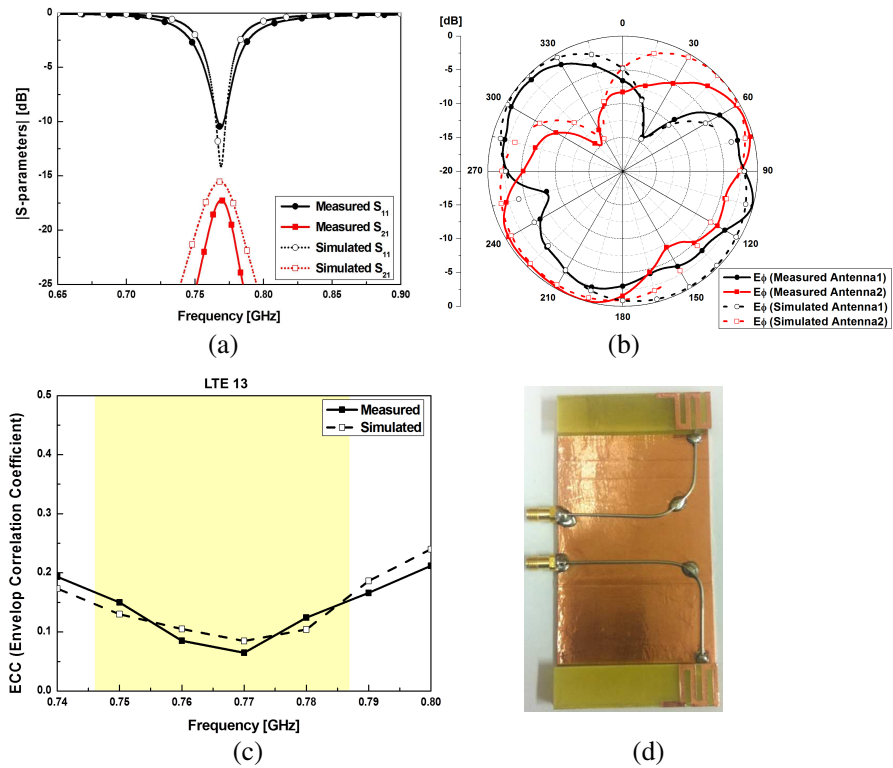


Figure 3. Simulated and measured results of LTE MIMO antenna: (a) S -parameters, (b) radiation pattern at 775 MHz (XY -plane), (c) ECC, and (d) photo of fabricated MIMO antenna.

Figure 4 shows the simulated reflection coefficients and isolations of the proposed MIMO antenna for different lengths (L_3) of Radiator 2 (inverted-L shaped structure). The isolation can be easily controlled and improved by adjusting the length (L_3) of Radiator 2. Greater isolation is obtained with the optimum length of $0.0625\lambda_0$ (27 mm) at 750 MHz. However, the length of the additional coupling element in previous studies [9, 10], which does not affect the resonant frequency, is approximately $0.25\lambda_g$ in order to reduce mutual coupling between the MIMO antennas. In this section, we propose a compact LTE 13 band MIMO antenna with a new configuration where the antenna elements are separately located on the top and bottom portions of a mobile handset to enhance the isolation between them while achieving a diagonally orthogonal radiation pattern by controlling the current path on the ground plane.

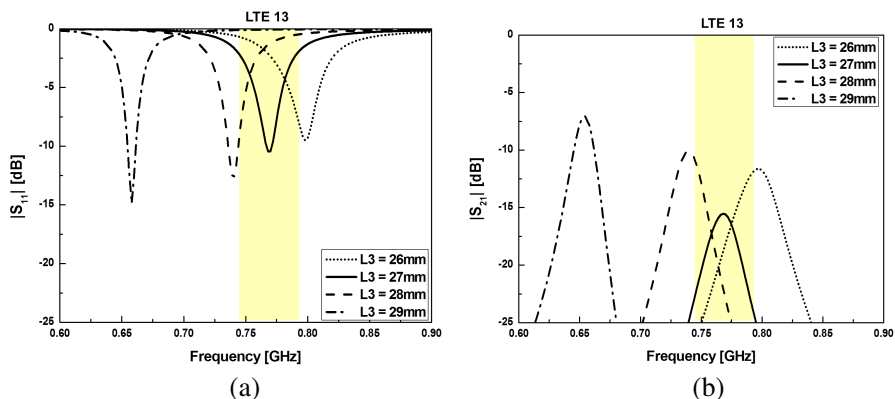


Figure 4. Simulated S -parameters for different lengths (L_3) of Radiator 2: (a) S_{11} and (b) S_{21} .

3. COMPACT TWO ANTENNAS FOR MIMO AND MULTIBAND OPERATIONS

In this section, based on a new configuration of the LTE 13 band MIMO antenna proposed in the previous Section 2, we finally propose two compact antennas for MIMO and multiband operations. The operating frequency bands of Antenna 1 located on the top portion and Antenna 2 located on the bottom portion include the LTE 13 (746 ~ 787 MHz)/DCS/PCS/UMTS (1710 ~ 2170 MHz) bands and the LTE 13 (746 ~ 787 MHz)/GSM850/900 (824 ~ 960 MHz) bands, respectively.

Figure 5 shows the geometry and photo of the proposed antenna. The overall dimensions of the proposed Antenna 1 and Antenna 2 mounted on a FR-4 ($\epsilon_r = 4.4$, loss tangent = 0.02) substrate are $48 \times 15 \times 6 \text{ mm}^3$ and $60 \times 15 \times 6 \text{ mm}^3$, respectively. The size of the ground plane is $60 \times 90 \times 1 \text{ mm}^3$, which corresponds to the 4.3 inch display size of a smart phone. Antenna 1 consists of Radiator 1a, Radiator 1b, and Radiator 1c, and Antenna 2 consists of Radiator 2a and Radiator 2b.

Figure 6 shows the surface current distribution of Antenna 1. Antenna 1 is mounted on the top of a mobile handset with three radiators (Radiator 1a, Radiator 1b, and Radiator 1c) by controlling the current path on the ground plane. Based on Section 2, Radiator 1a (meander line PIFA structure) in conjunction with Radiator 1b (Inverted-L shaped structure) covers the LTE 13 (746 ~ 787 MHz) band as shown in Figure 6(a). The overall length ($L_4 + L_5 + L_6$) of Radiator 1a and Radiator 1b is around $0.5\lambda_g$ (160 mm) at 775 MHz. As mentioned in Section 2, by achieving the orthogonal ground current

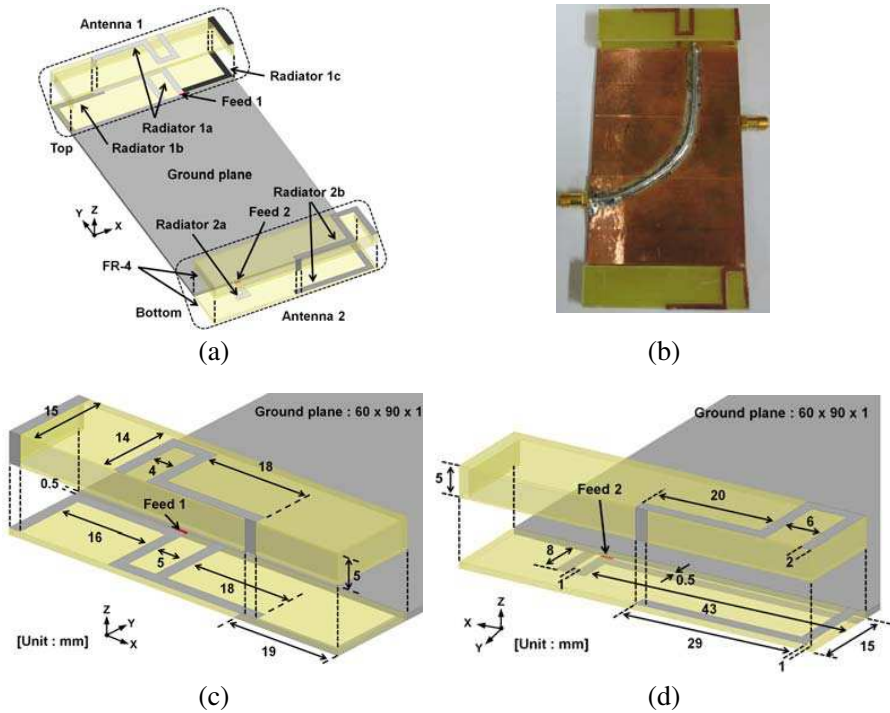


Figure 5. Geometry of proposed antenna: (a) Overall view of proposed antenna, (b) photo of fabricated antenna, (c) detailed dimensions of Antenna 1, and (d) detailed dimensions of Antenna 2.

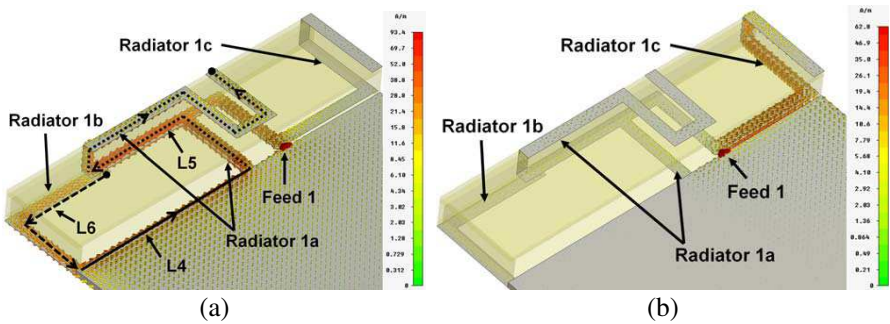


Figure 6. Surface current distribution of Antenna 1: (a) at 775 MHz and (b) at 1.8 GHz.

path with respect to that from Antenna 2, the mutual coupling between the LTE MIMO antenna elements can be reduced. To cover the additional DCS/PCS/UMTS (1710 ~ 2170 MHz) bands, Radiator 2c

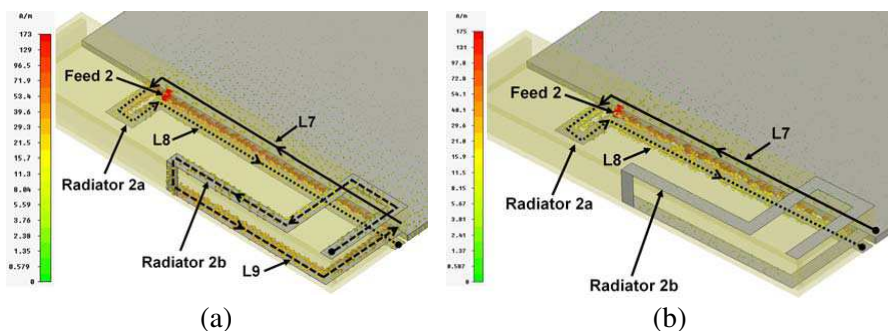


Figure 7. Surface current distribution of Antenna 2: (a) at 775 MHz and (b) at 900 MHz.

resonated at 1.8 GHz is added as shown in Figure 6(b).

Figure 7 shows the surface current distribution of Antenna 2. Antenna 2 is mounted on the bottom of a mobile handset with two radiators (Radiator 2a and Radiator 2b) by controlling the current path on the ground plane. Radiator 2a in conjunction with Radiator 2b covers the LTE 13 (746 ~ 787 MHz) band as shown in Figure 7(a). Radiator 2a is capacitively coupled to Radiator 2b. The overall length ($L_7 + L_8 + L_9$) of Radiator 1a and Radiator 1b is around $0.5\lambda_g$ (183 mm) at 775 MHz. The ground current path from Antenna 2 is also diagonally orthogonal to that of Antenna 1. Figure 7(b) shows the surface current distribution at 900 MHz where the resonant length of Radiator 2a is about $0.25\lambda_g$. When Antenna 2 operates at 900 MHz, Radiator 2a acts as $0.25\lambda_g$ PIFA which covers the additional GSM850/900 (824 ~ 960 MHz) bands.

Figure 8(a) shows the simulated and measured S -parameters of proposed antennas. Antenna 1 ($VSWR < 3$) can cover all of the LTE 13 (746 ~ 787 MHz)/DCS/PCS/UMTS (1710 ~ 2170 MHz) bands, and Antenna 2 ($VSWR < 3$) can operate for all of the LTE 13 (746 ~ 787 MHz)/GSM850/900 (824 ~ 960 MHz) bands. The measured isolation is greater than 14 dB, and this is generally acceptable for practical MIMO antenna applications in the industry. The proposed antenna has a total efficiency of greater than 40 % for all operating frequency bands as shown in Figure 8(b). Figure 8(c) shows the simulated and measured radiation patterns at 775 MHz. It is noticed that the polarizations of the two antennas are orthogonal to each other. Therefore, these orthogonal radiation patterns and high isolation (> 14 dB) give the lower ECC (< 0.25) for the entire LTE 13 band, which is much less than the recommend value of 0.5, as shown in Figure 8(d).

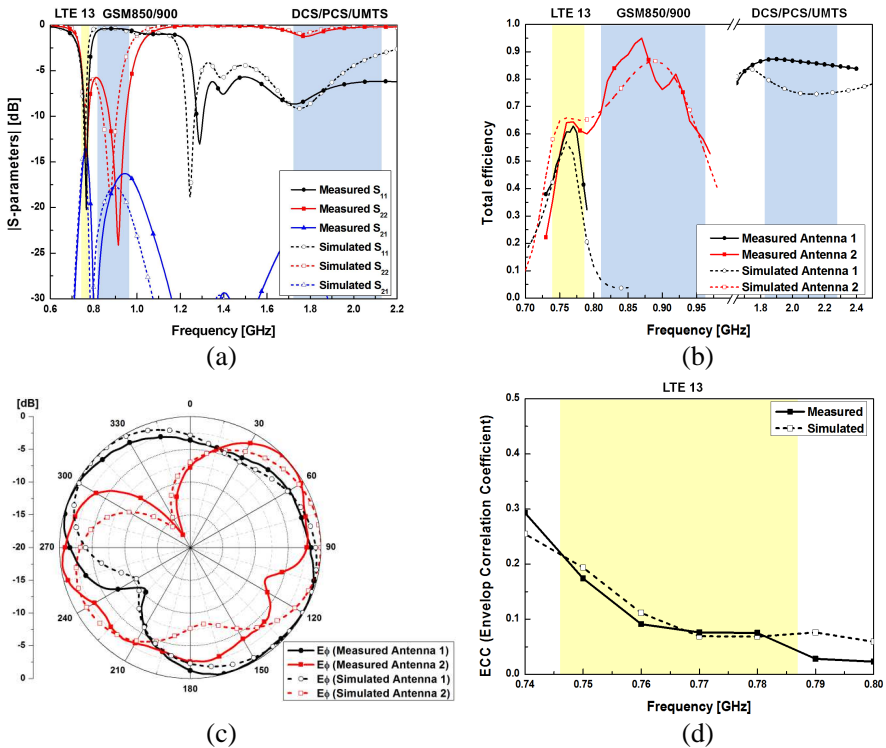


Figure 8. Simulated and measured results of proposed antennas: (a) S -parameters, (b) total efficiency, (c) radiation pattern at 775 MHz (XY -plane), and (d) ECC.

4. CONCLUSION

In this paper, we propose a new configuration of compact broadband antennas for LTE MIMO and multiband operations where antenna elements are separately located on the top and bottom portions of a mobile handset to enhance the isolation between them by achieving diagonally orthogonal radiation pattern while controlling the current path on the ground plane. High isolation (> 14 dB) and low ECC (< 0.25) between the MIMO antennas for the LTE 13 band are achieved. Antenna 1 and Antenna 2 can cover the LTE 13 (746 ~ 787 MHz)/DCS/PCS/UMTS (1710 ~ 2170 MHz) bands and the LTE 13 (746 ~ 787 MHz)/GSM850/900 (824 ~ 960 MHz) bands, respectively.

ACKNOWLEDGMENT

The present research was supported by a research grant from Kwangwoon University in 2013, and this work (Grants No. C0015229) was supported by Business for Cooperative R&D between Industry, Academy, and Research Institute funded Korea Small and Medium Business Administration in 2012.

REFERENCES

1. Yu, X. H., L. Wang, H.-G. Wang, X. Wu, and Y.-H. Shang, "A novel multiport matching method for maximum capacity of an indoor MIMO system," *Progress In Electromagnetics Research*, Vol. 130, 67–84, 2012.
2. Sharawi, M. S., A. B. Numan, and D. N. Aloï, "Isolation improvement in a dual-band dual-element MIMO antenna system using capacitively loaded loops," *Progress In Electromagnetics Research*, Vol. 134, 247–266, 2013.
3. Krairiksh, M., P. Keowsawat, C. Phongcharoenpanich, and S. Kosulvit, "Two-probe excited circular ring antenna for MIMO application," *Progress In Electromagnetics Research*, Vol. 97, 417–431, 2009.
4. Lee, J.-H. and C.-C. Cheng, "Spatial correlation of multiple antenna arrays in wireless communication systems," *Progress In Electromagnetics Research*, Vol. 132, 347–368, 2012.
5. Yoon, C., S.-G. Hwang, G.-C. Lee, W.-S. Kim, H.-C. Lee, C.-H. Lee, and H.-D. Park, "A frequency-selecting technique for mobile handset antennas based on capacitance switching," *Progress In Electromagnetics Research*, Vol. 138, 99–113, 2013.
6. Kusuma, A. H., A.-F. Sheta, I. M. Elshafiey, Z. Siddiqui, M. A. S. Alkanhal, S. Aldosari, S. A. Alshebeili, and S. F. Mahmoud, "A new low SAR antenna structure for wireless handset applications," *Progress In Electromagnetics Research*, Vol. 112, 23–40, 2011.
7. Zhao, K., S. Zhang, Z. Ying, T. Bolin, and S. He, "Reduce the hand-effect body loss for LTE mobile antenna in CTIA talking and data modes," *Progress In Electromagnetics Research*, Vol. 137, 73–85, 2013.
8. Harrington, R. F. and J. R. Mautz, "Theory of characteristic modes for conducting bodies," *IEEE Trans. Antennas Propag.*, Vol. 19, No. 5, 622–628, 1971.
9. Mak, A. C. K., C. R. Rowell, and R. D. Murch, "Isolation

- enhancement between two closely packed antennas,” *IEEE Trans. Antennas Propag.*, Vol. 56, No. 6, 3411–3419, 2008.
10. Chou, H.-T., H.-C. Cheng, H.-T. Hsu, and L.-R. Kuo, “Investigations of isolation improvement techniques for multiple input multiple output (MIMO) WLAN portable terminal applications,” *Progress In Electromagnetics Research*, Vol. 85, 349–366, 2008.
 11. Cui, S., S. X. Gong, Y. Liu, W. Jiang, and Y. Guan, “Compact and low coupled monopole antennas for MIMO system applications,” *Journal of Electromagnetic Waves and Applications*, Vol. 25, Nos. 5–6, 703–712, 2011.
 12. Gong, Q., Y.-C. Jiao, and S.-X. Gong, “Compact MIMO antennas using a ring hybrid for WLAN applications,” *Journal of Electromagnetic Waves and Applications*, Vol. 25, Nos. 2–3, 431–441, 2011.
 13. Li, J. F. and Q. X. Chu, “A compact dual-band MIMO antenna of mobile phone,” *Journal of Electromagnetic Waves and Applications*, Vol. 25, Nos. 11–12, 1577–1586, 2011.
 14. Islam, M. T. and M. S. Alam, “Compact EBG structure for alleviating mutual coupling between patch antenna array elements,” *Progress In Electromagnetics Research*, Vol. 137, 425–438, 2013.
 15. Diallo, A., C. Luxey, P. L. Thuc, R. Staraj, and G. Kossiavas, “Study and reduction of the mutual coupling between two mobile phone PIFAs operating in the DCS1800 and UMTS bands,” *IEEE Trans. Antennas Propag.*, Vol. 54, No. 11, 3063–3074, 2006.
 16. Chen, Z., Y.-L. Ban, J.-H. Chen, J. L.-W. Li, and Y.-J. Wu, “Bandwidth enhancement of LTE/WWAN printed mobile phone antenna using slotted ground structure,” *Progress In Electromagnetics Research*, Vol. 129, 469–483, 2012.
 17. Ban, Y.-L., J.-H. Chen, S.-C. Sun, J. L.-W. Li, and J.-H. Guo, “Printed wideband antenna with chip capacitor-loaded inductive strip for LTE/GSM/UMTS WWAN wireless USB dongle applications,” *Progress In Electromagnetics Research*, Vol. 128, 313–329, 2012.
 18. Chiu, C.-W., C.-H. Chang, and Y.-J. Chi, “Multiband folded loop antenna for smart phones,” *Progress In Electromagnetics Research*, Vol. 102, 213–226, 2010.
 19. Chen, Z., Y.-L. Ban, S.-C. Sun, and J. L.-W. Li, “Printed antenna for penta-band WWAN tablet computer application using embedded parallel resonant structure,” *Progress In Electromagnetics Research*, Vol. 136, 725–737, 2013.

20. Sze, J.-Y. and Y.-F. Wu, "A compact planar hexa-band internal antenna for mobile phone," *Progress In Electromagnetics Research*, Vol. 107, 413–425, 2010.
21. Liao, W.-J., S.-H. Chang, and L.-K. Li, "A compact planar multiband antenna for integrated mobile devices," *Progress In Electromagnetics Research*, Vol. 109, 1–16, 2010.
22. Li, P., J. Pan, D. Yang, Z.-P. Nie, and J. Xing, "A novel quad-band (GSM850 to IEEE 802.11a) PIFA for mobile handset," *Progress In Electromagnetics Research*, Vol. 137, 539–549, 2013.
23. Gujral, M., J. L.-W. Li, T. Yuan, and C.-W. Qiu, "Bandwidth improvement of microstrip antenna array using dummy EBG pattern on feedline," *Progress In Electromagnetics Research*, Vol. 127, 79–92, 2012.
24. Monavar, F. M. and N. Komjani, "Bandwidth enhancement of microstrip patch antenna using jerusalem cross-shaped frequency selective surfaces by invasive weed optimization approach," *Progress In Electromagnetics Research*, Vol. 121, 103–120, 2011.
25. Vongsack, S., C. Phongcharoenpanich, S. Kosulvit, K. Hamamoto, and T. Wakabayashi, "Unidirectional antenna using two-probe excited circular ring above square reflector for polarization diversity with high isolation," *Progress In Electromagnetics Research*, Vol. 133, 159–176, 2013.
26. Xu, H.-X., G.-M. Wang, and M.-Q. Qi, "A miniaturized triple-band metamaterial antenna with radiation pattern selectivity and polarization diversity," *Progress In Electromagnetics Research*, Vol. 137, 275–292, 2013.
27. Kalliola, K., K. Sulonen, H. Laitinen, O. Kivekäs, J. Krogerus, and P. Vainikainen, "Angular power distribution and mean effective gain of mobile antenna in different propagation environments," *IEEE Trans. Antennas Propag.*, Vol. 51, No. 5, 823–838, 2002.
28. Chen, X., "Measurements and evaluations of multi-element antennas based on limited channel samples in a reverberation chamber," *Progress In Electromagnetics Research*, Vol. 131, 45–62, 2012.
29. Lee, J.-H. and C.-C. Cheng, "Spatial correlation of multiple antenna arrays in wireless communication systems," *Progress In Electromagnetics Research*, Vol. 132, 347–368, 2012.
30. Li, P. and L. Jiang, "The far field transformation for the antenna modeling based on spherical electric field measurements," *Progress In Electromagnetics Research*, Vol. 123, 243–261, 2012.